


## ORIGINAL ARTICLE

# Guided bone regeneration using titanium mesh to augment 3-dimensional alveolar defects prior to implant placement. A pilot study

Giuseppe Lizio<sup>1</sup>  | Gerardo Pellegrino<sup>1</sup> | Giuseppe Corinaldesi<sup>1</sup> | Agnese Ferri<sup>1</sup> | Claudio Marchetti<sup>2</sup> | Pietro Felice<sup>1</sup>

<sup>1</sup>Unit of Oral Surgery, Department of Biomedical and Neuromotor Sciences (DIBINEM), University of Bologna, Bologna, Italy

<sup>2</sup>Unit of Maxillofacial Surgery, Department of Biomedical and Neuromotor Sciences (DIBINEM), University of Bologna, Bologna, Italy

**Correspondence**

Giuseppe Lizio, Unit of Oral Surgery, Department of Biomedical and Neuromotor Science (DIBINEM), University of Bologna, Via San Vitale 59, 40125 Bologna, Italy.  
Email: [giuseppelizio@libero.it](mailto:giuseppelizio@libero.it)

**Abstract**

**Objectives:** To evaluate the outcomes of bone regeneration using a customized titanium mesh scaffold to cover a bone graft for reconstruction of complex defects of the jaws.

**Materials and Methods:** 19 large defects were digitally reconstructed using CT scans according to the prosthetic requirements. A titanium mesh scaffold was designed to cover the bone (autologous/bovine bone particulate) graft. At least 6 months after surgery, a new cone-beam CT was taken. The pre- and postoperative CT datasets were then converted into three-dimensional models and digitally aligned. The actual mesh position was compared to the virtual position to assess the reliability of the digital project. The reconstructed bone volumes (RBVs) were calculated according to the planned bone volumes (PBVs), outlining the areas under the mesh. These values were then correlated with the number of exposures, locations of atrophy, and virtually planned bone volume.

**Results:** The mean matching value between the planned position of the mesh and the actual one was  $82 \pm 13.4\%$ . 52.3% (40% early and 60% late) exposures were observed, with 15.8% exhibiting infection. 26.3% resulted as failures. The amount of reconstructed bone volume (RBV) in respect to PBV was  $65 \pm 40.5\%$ , including failures, and  $88.2 \pm 8.32\%$  without considering the failures. The results of the exposure event were statistically significant ( $p = .006$ ) in conditioning the bone volume regenerated.

**Conclusions:** This study obtained up to 88% of bone regeneration in 74% of the cases. The failures encountered (26%) should underline the operator's expertise relevance in conditioning the final result.

**KEYWORDS**

GBR, titanium meshes, virtual planning

The trial has been registered and published in *ClinicalTrials.gov* (ID: NCT04942223).

This is an open access article under the terms of the [Creative Commons Attribution-NonCommercial-NoDerivs](https://creativecommons.org/licenses/by-nc-nd/4.0/) License, which permits use and distribution in any medium, provided the original work is properly cited, the use is non-commercial and no modifications or adaptations are made.

© 2022 The Authors. *Clinical Oral Implants Research* published by John Wiley & Sons Ltd.

## 1 | INTRODUCTION

The implant-borne rehabilitation of three-dimensional and extended alveolar defects is not simple in any case. Anatomic and prosthetic demands that are not resolved using short or tilted implants require bone reconstruction (Chiapasco et al., 2009; Lizio et al., 2014). Therefore, a versatile regenerative technique is crucial in treating such sites impaired in thickness and height or with irregular morphologies, covered by thin and poorly keratinized soft tissues prone to dehiscence (Lizio et al., 2016; Sanz et al., 2019).

Currently, we can virtually simulate the entire treatment process, transferring the CT data to dedicated software and designing the missing hard tissue based on the prosthetic project and the consequent features and positions of the implants (Ciocca et al., 2015, 2018). The bone engineering techniques can involve printing bioinert synthetic scaffolds, fitting the defect with osteoconductive or osteoinductive potentialities (Bartnikowski et al., 2020; Jacotti et al., 2014). However, considering the autologous bone as the better choice for atrophic sites and the necessity to transfer the virtual volumetric and morphologic project to the graft for the entire healing period, the guided bone regeneration (GBR) with preformed titanium meshes was taken into consideration (Ciocca et al., 2015, 2018; Cucchi et al., 2020; Maiorana et al., 2001). The design and printing of a customized device, designed to simulate the ideal reconstruction, eliminates the intra-operative handling and trimming, reducing surgical time and minimizing stress for the soft tissues when compared to traditional meshes. This also applies to regular and rounded edges due to the advanced 3D laser-sintering printing technology (Chiapasco et al., 2021; Ciocca et al., 2015, 2018; Sumida et al., 2015). This customized GBR can reduce the risk of dehiscence, positively correlated to the amount of planned bone volume and the consequent soft tissue stress (Lizio et al., 2014). Limiting as much as due to the alveolar reconstruction, and standardize the reconstructive procedure, which is usually more dependent on the operator's skills. With traditional manually created titanium meshes, the exposure range is extensive (0–68.9%) (Lizio et al., 2014; Pieri et al., 2008; Poomprakobsri et al., 2021). Ciocca et al., using digitally customized meshes, reported 66% of postoperative exposure morbidity in nine cases (Ciocca et al., 2018), and Li et al. reported 25% morbidity in 16 patients (Li et al., 2021); Chiapasco et al. reported 11 exposure cases in 53 dehiscence cases (Chiapasco et al., 2021), and Cucchi et al. recorded one in 10 cases (Cucchi et al., 2020). Sumida et al., comparing two groups of 13 patients, found one and three exposures for CAD/CAM and traditional devices, respectively (Sumida et al., 2015). A recent meta-analysis stated exposure rates of 31% with custom-made meshes and 51% with conventional meshes (Zhou et al., 2021). Comparing the actual bone volumes with digitally planned bone volumes from CAD/CAM procedures, Cucchi et al. and Chiapasco et al. reported technique reliability rates of 89% and 91.9%, respectively (Chiapasco et al., 2021; Cucchi et al., 2020). These results are consistent with Li et al., recording 95.82% reliability (range: 88.53%–99.15%) (Pellegrino et al., 2021), but higher than Lizio et al., with a 69.8% of obtained bone, both using meshes

performed on stereo-lithographic models (Lizio et al., 2014). The literature on the GBR with customized meshes is at an early stage and thus presents a few shortcomings. Besides no-clearness regarding the starting extension of the deficits, the limited number of cases reported and the questionable evaluation methods of the bone gain can confuse the scenario. The preimplant phase predictability of a virtually planned GBR depends on the thoroughness and accuracy of the project's bone volume and exposure rate data, as some studies reported the obtained bone gain without comparing it to the planned values (Ciocca et al., 2018; Sagheb et al., 2017). Volumetric measurements for three-dimensional defects should be adopted more often than linear, primarily when not performed in correspondence of the implant sites (Sagheb et al., 2017). The intra-operative fitting of the mesh should be evaluated as a presumption of the reliability of the procedure (Li et al., 2021).

The present trial aims to understand the use of customized titanium meshes to reconstruct complex and extended defects in terms of bone gain and exposure percentage, compared to the traditional manual approach.

## 2 | MATERIALS AND METHODS

Seventeen patients, five male and 12 female, with a mean age of 55.9 ( $\pm 13.7$ ), were recruited from July 2013 to November 2017. The patients had a total of 19 complex three-dimensional defects involving the alveolar ridge of maxillary and mandibular edentulous areas. After completing the follow-up, these patients were considered in this prospective prosthetic-guided computerized bone regeneration protocol. The project implied a virtual bone defect reconstruction related to the implant-borne prosthetic demands. A laser-sintering-printed titanium mesh worked as a scaffold for containing and modeling the particulate bone taken from the intraoral donor sites. The Ethics Committee of S. Orsola-Malpighi University Hospital, Bologna, Italy, approved the study (approval No. 121/2013/O/Disp). The study's primary outcome was that the evaluation of the bone volume regeneration, compared with virtually planned bone volume, demonstrated an acceptable level of superimposition between the virtual and intra-operative mesh fitting. The secondary outcome was to record the mesh exposures and their association with the level of bone regeneration.

All patients fulfilled the general inclusion criteria, consisting of the absence of any systemic or local contraindication to surgical treatment (i.e., acute or chronic infections in the head and neck; smoking >10 cigarettes per day; uncontrolled diabetes (glycated hemoglobin level >7 mg/dl); a history of radiation therapy in the head or neck region; current anti-tumor chemotherapy; liver, blood, or kidney disease; immunosuppression; everyday corticosteroid use; pregnancy; inflammatory and autoimmune disease of the oral cavity; and poor oral hygiene and motivation). The specific conditions for intervention were the presence of maxillary or mandibular complex defects (with horizontal and vertical deficits in the same site), which was considered inadequate for the placement of at least two

standard fixtures ( $\geq 6$  mm long and  $\geq 3.3$  wide). Nineteen bone deficits were treated: eight in maxillae (one posterior, associated with sinus lift, and seven anterior) and 11 in posterior mandibles. Five upper jaws with complete edentulism were treated with bilateral sinus lifts performed with a lateral approach (Table 1).

## 2.1 | Virtual planning

The Digital Imaging and Communication in Medicine (DICOM) data and the STL (3D scan) files of intraoral, extraoral and laboratory scanning were paired in a software platform to plan rehabilitation according to anatomic and prosthetic demands. In all cases, the project was performed by an experienced dental prosthodontist

in collaboration with the oral surgeon in charge. Each site for implants of at least 8 mm  $\times$  3 mm were evaluated. The total number of planned implants was 63. The project data were imported into the software (Mimics Innovation Suite, v17; Materialise) for obtaining the three-dimensional models of the jaws (maxilla or mandible) by segmentation, maintaining the same threshold values. The mandibular models also included the reproduction of the inferior alveolar nerve. The maxillary models included the alveolar process, the maxillary sinuses, and the pterygoid and zygomatic processes. Subsequently, the plan was exported into CAD software (Freeform Modelling Plus, version 13.0, 3D Systems) to design the minimum bone augmentation required (a 5 mm safety zone around each implant was assumed) and an over contouring of 1.5 mm thickness, simulating the periosteum-like tissue.

TABLE 1 Demographic and descriptive data of the patients (Pts)

Pts	Sites	Gender	Age(Y)	Maxilla (0) Mandible (1)	Anterior (0) Posterior (1)	Exposure yes (0) Exposure no (1)	Total edentulism (0) Partial edentulism (1) Intermediate edentulism (2)
1	1	1	51	1	1	1	1 (Missing teeth: 44,45,46,47)
2	2	0	72	0	1	0	1 (Missing teeth: 14,15,16,17)
3	3	1	64	1	1	0	1 (Missing teeth: 34,35,36,37)
4	4	1	68	1	1	0	1 (Missing teeth: 45,46,47)
5	5	0	58	0	0	0	0
6	6	0	59	0	0	1	0
7	7	1	57	1	1	1	1 (Missing teeth: 35,36,37)
8	8	0	46	0	0	0	0
9	9	1	45	1	1	1	1 (Missing teeth: 45,46,47)
9	10	1	45	1	1	0	1 (Missing teeth: 36,37)
10	11	1	25	1	1	1	2 (Missing teeth: 35,36)
10	12	1	25	1	1	0	2 (Missing teeth: 45,46)
11	13	1	55	0	0	0	2 (Missing teeth: 21,22,23,24,25,26)
12	14	1	76	1	1	1	1 (Missing teeth: 33,34,35,36,37)
13	15	1	62	1	1	1	1 (Missing teeth: 34,35,36,37)
14	16	1	69	1	1	1	1 (Missing teeth: 46,47)
15	18	1	63	0	0	1	0
16	19	1	50	0	0	0	0
17	20	0	31	0	0	0	2 (Missing teeth: 11,12,13)

Further, the mesh was designed to cover the calculated volumes, calibrated at 0.1–0.5 mm thickness, with rounded edges fitting the defect borders and the fixation hole position. The virtual mesh, saved in stereolithographic (STL) format, was finally reviewed by the designer, the prosthodontist, and the surgeon; then, once approved, the mesh was 3D-printed using an EOSINT M270 printer (Electro-Optical Systems) and digital machine laser sintering (DMLS). Finally, titanium Ti64 powder was melted to build a mesh with the necessary physical characteristics and biocompatibility (Figures 1 and 2).

## 2.2 | Surgical procedure

The surgical procedures were performed by four different surgeons with different expertise and experience on the same surgical and research team, all under general hospital anesthesia, except for three cases treated with local anesthesia on patients' explicit requests. The area to be treated was locally infiltrated with anesthetic using articaine hydrochloride 4% with epinephrine 1:100.000. The surgery started with a mid-crestal incision with vertical releasing cuts, followed by raising the full-thickness buccal and lingual/palatal flaps to expose the entire bone defect. The mental or infraorbital nerve emergence was then identified. The flaps were coronally extended to assure a complete closure with a passive suture above the titanium device by releasing incisions and dissection of the periosteum. Subsequently, an intraoral mandibular ramus bone cortical block was harvested; an enveloped mobile mucosa incision in the mandibular vestibule in the molar zone was made to reach the external oblique line, except for the posterior mandibular atrophies, where a single flap was designed to expose the defect and the donor site. The bone osteotomies, involving only the buccal cortex, were performed with piezo-surgery instruments to define a rectangular block of about 3.5 cm length, 1.5 cm height, and 4 mm thickness, eventually fractured with a chisel. The bone block was milled and mixed with deproteinized bovine bone (Bio-Oss, Geistlich Pharmaceutical) in a 60/40 ratio. The particulate graft was placed to fill the deficit above the mesh to reach perfect stability and unity with the defect's borders. Two or three titanium screws were used to stabilize the device, and the flaps were carefully sutured after determining that the surgical flaps could cover the augmented area (Figure 3).

Ceftriaxone (antibiotic) was administered intravenously on induction at a loading dose of 2 g, together with a non-steroidal analgesic (ibuprofen). This treatment was continued at an oral dose of 2 g beginning the day after surgery and continuing for 6 days. In the three cases treated in the office, 2 g of amoxicillin was administered orally 1 h before the intervention and continued for 6 days at 2 g. The patients were instructed to avoid brushing on the surgical site, follow a soft diet for 3 weeks, and maintain appropriate oral hygiene, including twice-daily rinsing with 0.2% chlorhexidine and applying 0.2% chlorhexidine gel to the wounds. Patients were

monitored monthly until the second-stage surgery during the postoperative healing period, and all complications were recorded. After at least 6 months of healing, a new cone-beam CT scan dataset was taken to verify the bone augmentation before implant surgery (Figure 4).

In the case of mesh exposure, its development progress and association with infection signs guided decisions about the early removal of the device. Thus, the mesh was removed in case of evident infection associated with early (<6 weeks) and wide (>0.5 cm<sup>2</sup>) exposure. Signs of infection were considered as the clear secretion of pus or the presence of a fistula associated with external overgrowth of reddish and bleeding tissue. The current situation was maintained after the first 6 months, except in the cases of late infection or soft tissue damage. Disinfection with chlorhexidine 0.2% and delicate site debridement were performed in the other situations. Implant placement was performed under local anesthesia. Titanium meshes and fixation screws were exposed and removed, and implant seating was completed according to the project (Figure 5).

## 2.3 | Evaluation parameters

### 2.3.1 | Complication rates

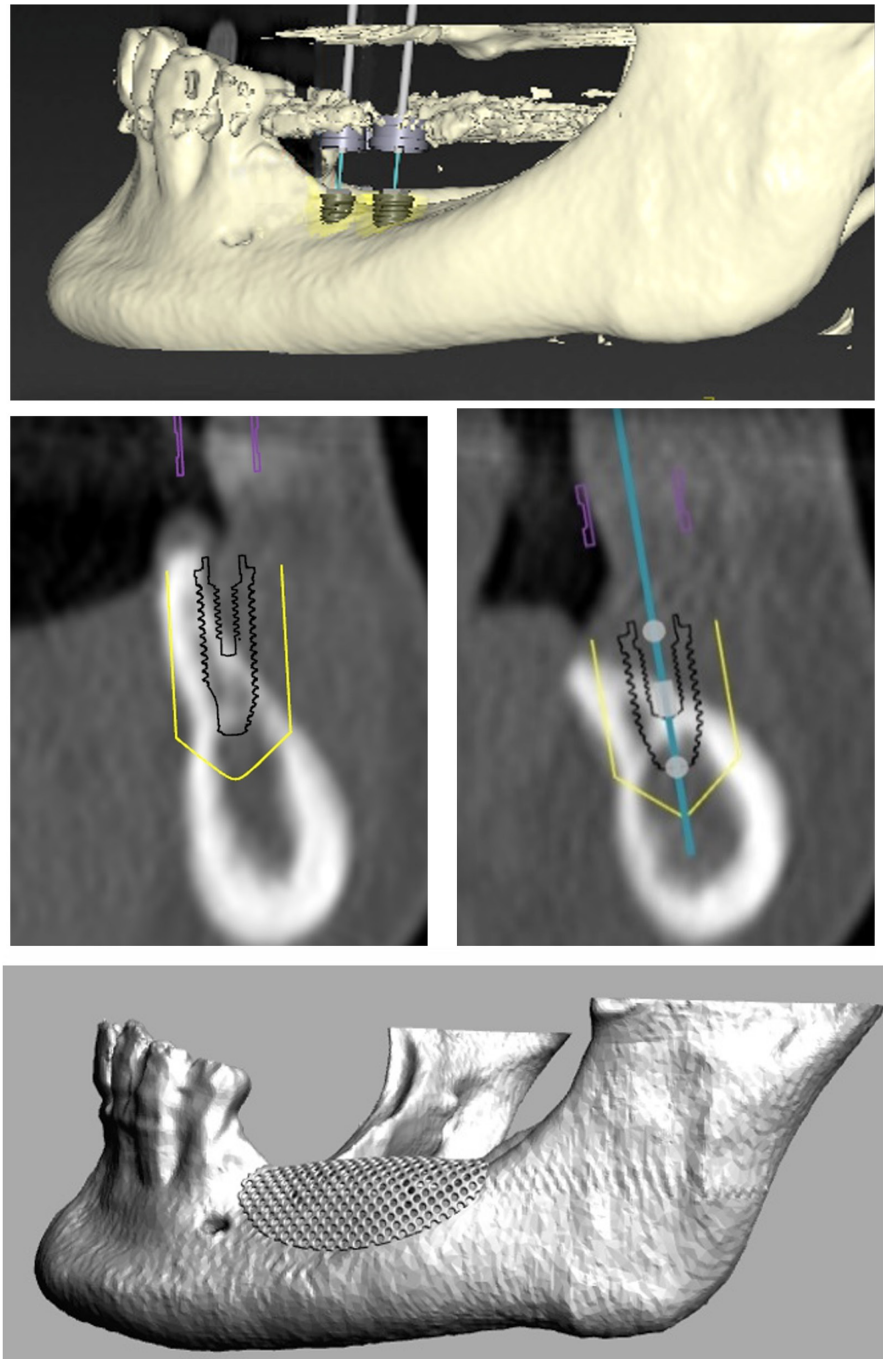
The number of exposures, the timing of their appearance, the presence of infection, and the early mesh removal were considered and correlated with the regenerated bone volumes.

### 2.3.2 | Mesh fitting evaluation

The DICOM data of the postoperative CT were imported into the three-dimensional modelling segmentation software used for the virtual project planning, and the volumes obtained after defining the total area under the meshes in all slices were digitally aligned with the virtual volumes. The difference, expressed in percentage values, evidenced the level of fitting that the meshes fulfilled (Figure 6). The evaluation was performed independently by two experts in informatics and virtual design. The interobserver discrepancy was minimal (<0.5 cm<sup>3</sup>), and the mean data were considered in the dataset.

Reconstructed Bone Volume (RBV) evaluation. The pre- and postoperative CT datasets were converted into 3D models using Amira imaging software (version 5.3.3, Visage Imaging GmbH). The segmentation required the jaw structure to have at least six precise anatomical matching points to perform the superimposition. Next, the pre- and postoperative models were digitally aligned in the reconstruction region using Geomagic Studio 12 software (Raindrop Geomagic Inc.). The measurements were performed after the alignment was verified at a minimum tolerance range of  $\pm 0.37$  mm in the areas not affected by the surgery. The space between the mesh profile and the basal bone in each slice was virtually selected and rendered to obtain the

**FIGURE 1** Preoperative virtual planning of the mesh design, according to implant positions and dimensions



*Planned Bone Volume (PBV)*. Based on the grayscale value of pixels in the images, the empty space area was rendered to determine the *Lacking Bone Volume (LBV)*. The selection of the representative areas for PBV and LBV was performed independently by two radiologists. The interobserver discrepancy was minimal ( $<0.5 \text{ cm}^3$ ), and the mean datum was considered in the dataset.

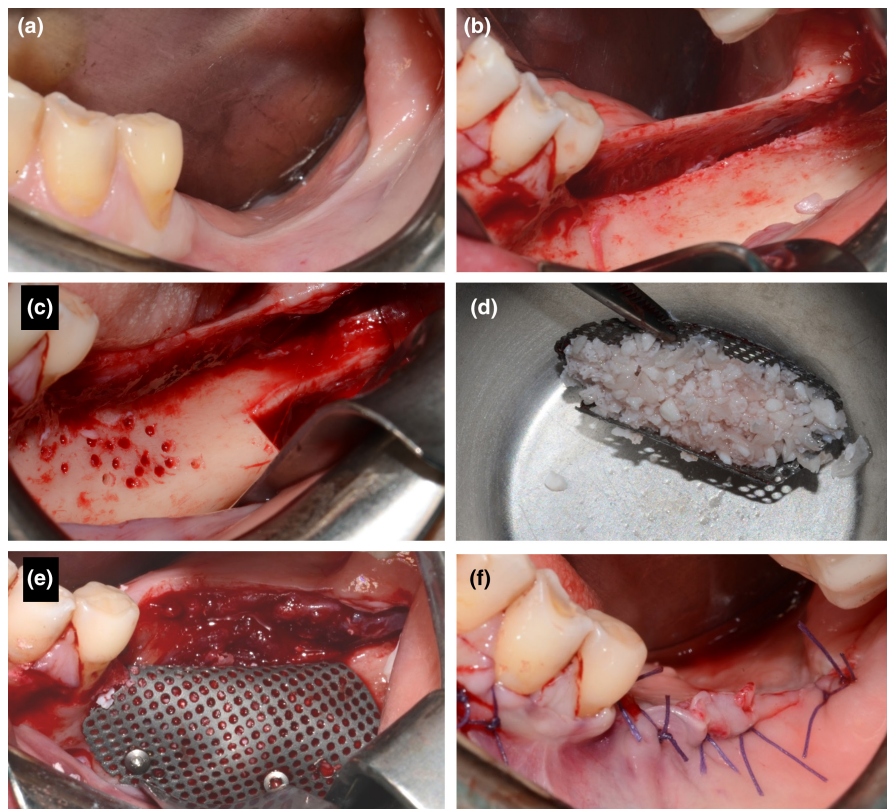
The *Reconstructed Bone Volume (RBV)* was derived by  $\text{PBV} - \text{LBV}$  (The lacking volume subtracted from the planned volume). In addition to the considered complications, RBV was correlated to the virtual-planned volumes and the defect locations (Figure 7).

Figure 6-8 show another case of mandibular atrophy.

## 2.4 | Statistical analysis

A descriptive analysis was performed presenting continuous variables as the mean  $\pm$  standard deviation (SD), following a normal distribution according to the Shapiro-Wilk  $W$  test; categorical variables were presented as absolute and relative frequencies.

A multiple regression model was defined for the reconstructed bone volume. Jaw site (anterior or posterior, mandibular or maxillary), mesh exposure, and infection occurrence were considered covariates. A paired  $t$ -test was used to compare the virtually planned volume, and the volume under the mesh placed just after the



**FIGURE 2** Operative surgical phases: starting clinical situation (a), osseous status after raising the flaps (b), block graft harvested from the mandibular ramus (c), mesh loaded with the particulate bone (d), fixation of the mesh (e), closure of soft tissue (f)

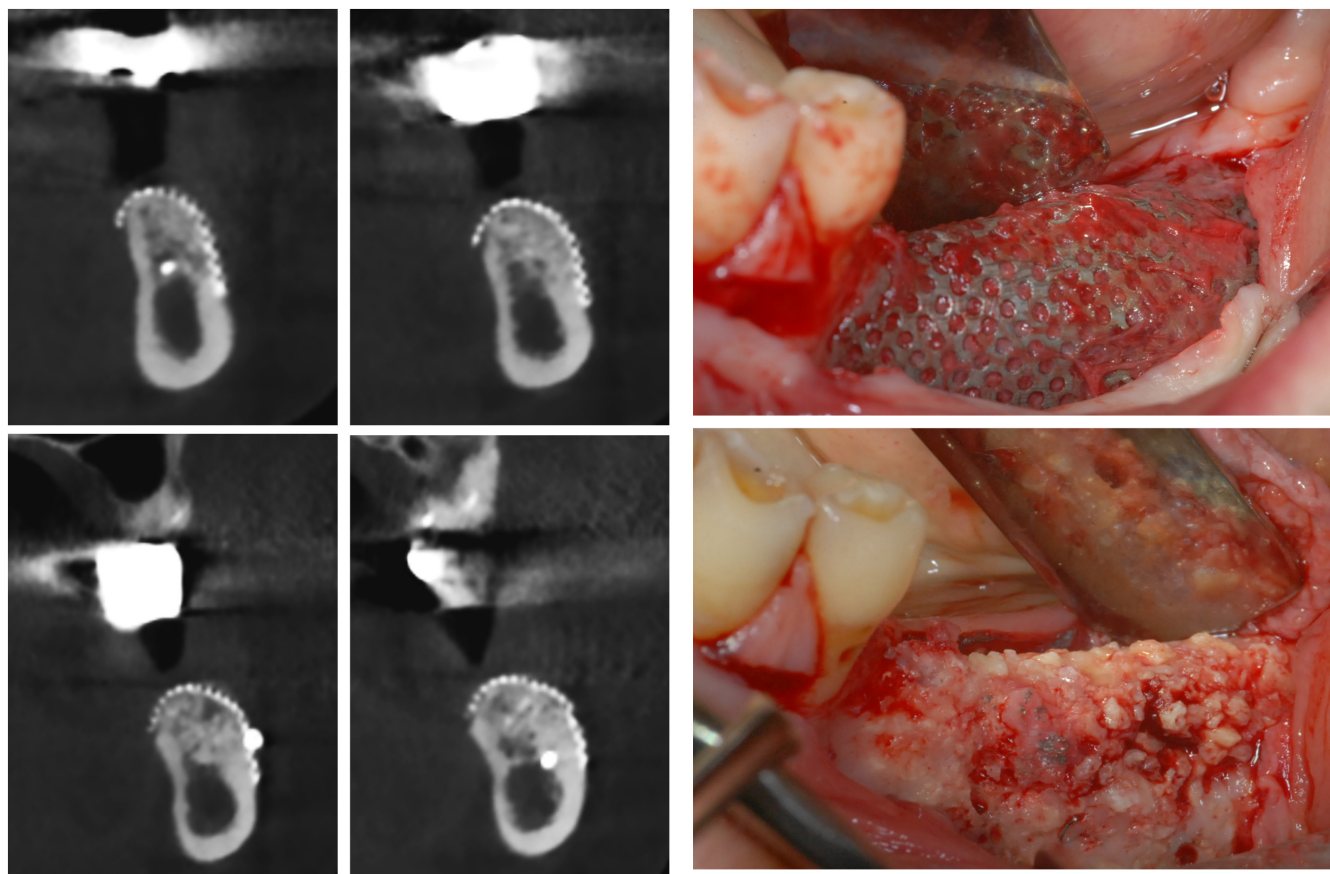
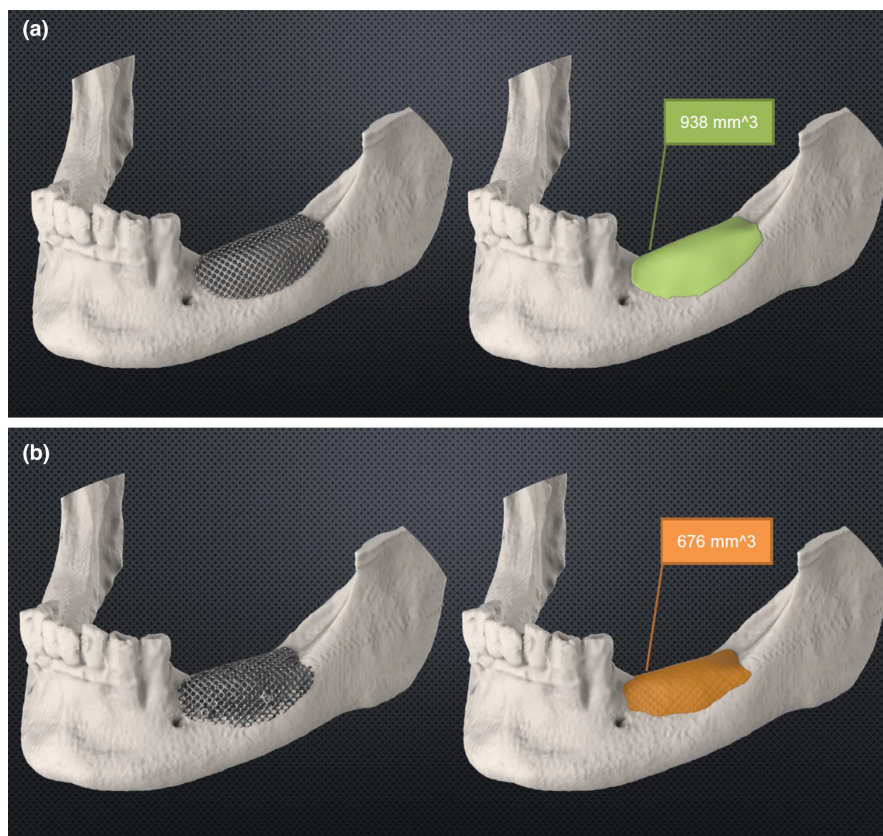


**FIGURE 3** Cross-sectional slices from the postoperative cone-beam CT before implant placement, and relative clinical situation at surgical re-entry

**FIGURE 4** Mesh fitting evaluation by comparing the 3d virtual mesh position (a) and the actual position (b) after importing the postoperative data



surgery. The significance level was set at 0.05. All the analyses were performed using Stata software (version 15, Stata Corp LP).

The authors state that this study is in compliance with the appropriate EQUATOR guidelines/checklist in Appendix S1.

### 3 | RESULTS

#### 3.1 | Complication rates

The overall number of exposures recorded was 10 (52.63%): six early (<6 weeks), and four late ( $\geq 6$  weeks), with an overall mean exposure time of  $9 \pm 8.43$  weeks: ( $3.6 \pm 1.36$  early and  $18.3 \pm 26.61$  late). Three infection events (15.79%) occurred, associated with exposures observed at 2, 5, and 8 weeks. Five sites (one edentulous maxilla and four posterior mandibles) completely lost the graft without reaching the implant placement phase (26.32% failure rate). Out of these unsuccessful sites, four had early exposures, of the meantime 4 weeks (range 2–5 weeks) post-surgery except for one, a complete maxillary edentulism, which presented dehiscence after 12 weeks. In these cases, the mesh was removed before 6 months of healing except for one case, in which the waiting period was extended to 11 months in the hopes of recovering the soft tissues. Regarding the other sites affected by dehiscence, four of five underwent a mesh removal before the implant placement, with no more than 2 months of waiting before the implant session. In one case, the implant insertion was performed contemporarily to the mesh removal.

In addition, two cases experienced an episodic tingling sensation at the inferior lip region, on the same side of the graft harvesting site, lasting more than 1 year after the intervention.

Apart from the failed cases, all sites underwent the implant placement phase without variations in the number and positions of the fixtures. Standard-dimension screws ( $\geq 8$  mm long and  $\geq 3.5$  mm wide) were placed in all cases.

#### 3.2 | Mesh fitting evaluation

Comparing the virtually planned mean bone volumes with the mean volumes under the meshes, an overall mean percentage of  $82 \pm 13.4$  mesh fitting resulted; the difference between planned and postoperative data was not statistically significant ( $p = .217$ ).

#### 3.3 | Reconstructed bone volume (RBV)

The *Planned Bone Volume* (PBV) mean value of  $1153.25 \pm 577.78$  mm<sup>3</sup>, lacking bone volume (LBV) mean values of  $149.33 \pm 177.59$  mm<sup>3</sup> and  $110.03 \pm 165.36$ , for including and excluding failures respectively, resulted in an RBV mean value of  $1003.92 \pm 465.79$  mm<sup>3</sup>. The RBV resulted in  $65.04\% \pm 40.55\%$  of the PBV, which increased to  $88.2 \pm 8.32\%$  when failures were excluded (Tables 2 and 3).

The univariate inferential association among RBV as the dependent variable found only the exposure events were relevant to the procedure ( $p = .006$ ), regardless of the appearance, infection,

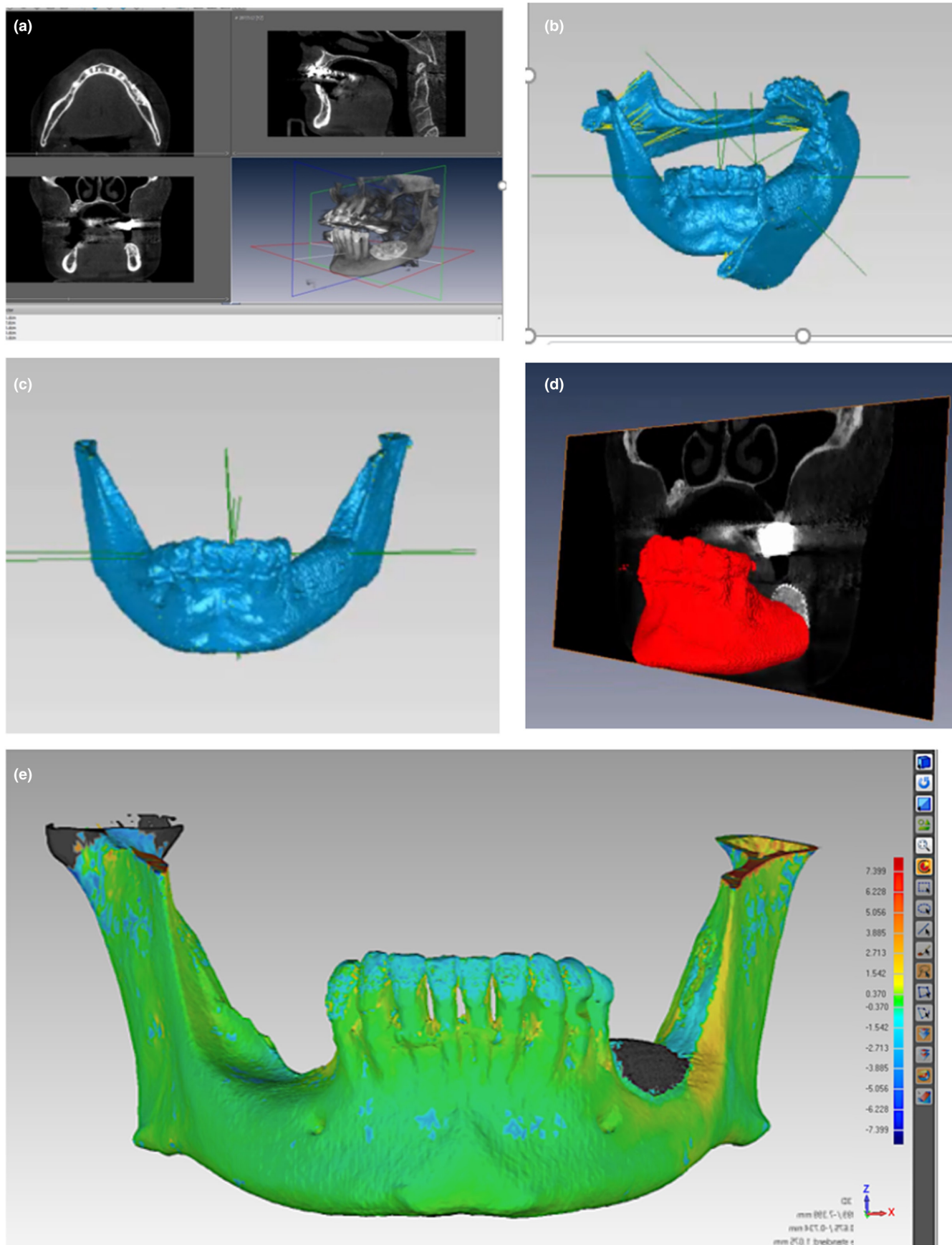
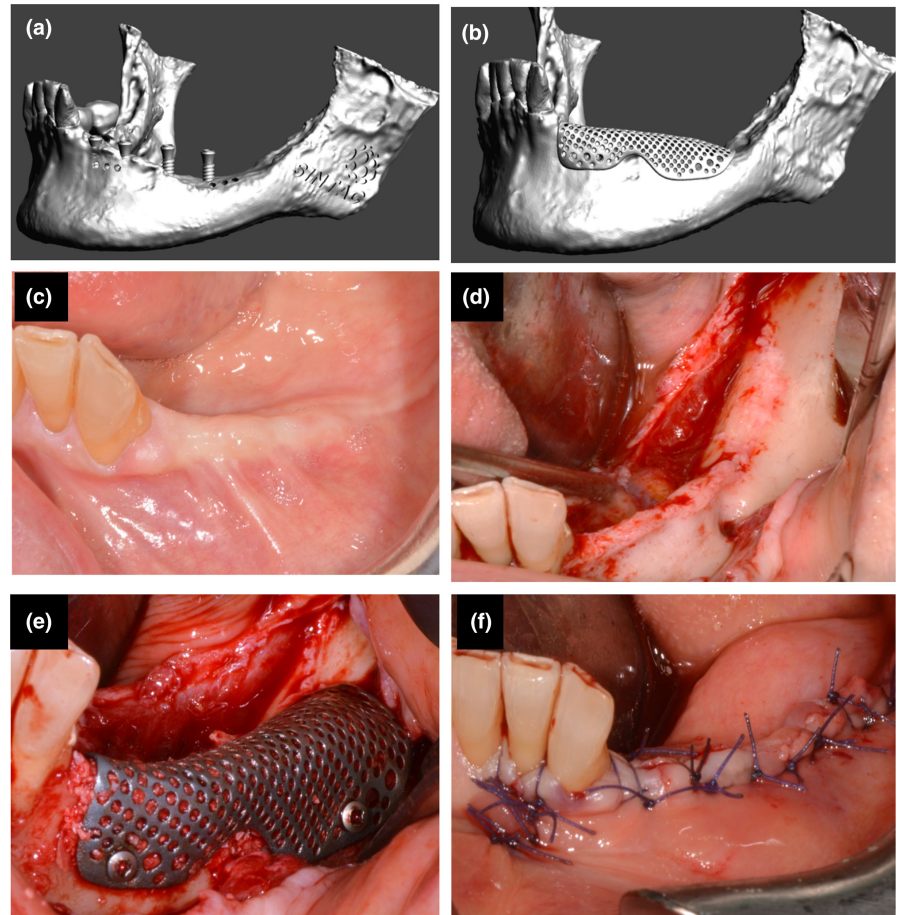


FIGURE 5 Segmentation procedure using Amira imaging software (a) and alignment of the 3D models (b, c, d, e) with Geomagic software for the volumetric evaluation



**FIGURE 6** Another case of left mandibular atrophy treated with the same protocol. Preoperative virtual planning of the mesh design (a, b) and operative surgical phases (c–f)



and mesh removal timing. The localization of the jaw and jaw area defects and the planned bone volume did not result in significant changes ( $p > .05$ ). The multivariate regression model, including the location of the defects (upper/lower jaw, anterior/posterior), the exposure and the infection events, confirmed that the mesh exposure occurring during the healing period is a predicting factor for higher values of RBV (Table 4).

Out of the 63 implants planned, 39 (61%) were placed. Regarding the 24 not inserted implants, 14 were related to the complete failed site. Eight implants were not placed for patients' dropouts due to personal and unexpected serious events. In particular, one patient moved away, one had to undergo radiotherapy for oncological pathology in the head and neck district, and one gave up for economic reasons. About the patients who adhered to the second phase, two implants in two patients were not placed for the quality/quantity of the regenerated bone.

All the 39 inserted fixtures were loaded as planned with screwed-connected fixed prostheses. The implant survival rate was 97.7%, with a mean of 30 (24–62.4) month follow-up from the prosthetic finalization. The mean rate of bone resorption was 1.96 (range 0.17–4.44) mm. This parameter was digitally calculated on the peripical x-rays at the end of follow-up, averaging the mesial and distal distance from the implant shoulder to the most coronal point of the bone level.

Graph 1 shows the patients' treatment flowchart.

## 4 | DISCUSSION

The prerequisite to understanding the usefulness of the digitized GBR was to check the mesh's fitting to the bone anatomy. Only one study in the literature focused on this issue (Li et al., 2021), adopting two evaluation methods after the superimposition of the preoperative model with virtually augmented the preimplant and postimplant models. Regarding the volumetric evaluation, these authors recorded an average volume value under the mesh in the post-GBR model of +19.3% than what was virtually planned preoperatively, perhaps due to an upward shifting of the device, resulting in a statistically significant difference on a sample of 16 sites (Li et al., 2021). Our trial detected a mean correspondence of 82% among the virtual volumes and those under the mesh in the postoperative CBCT, with lower average volumes of 18%. Even if not statistically significant, these data, with a range of values from 53.3% to 100%, should be an incentive better to address the problem of mesh fitting in future studies. As a second evaluation, Li et al. reported a mean value of  $0.59 \pm 0.47$  mm of mesh contour deviation among the virtual preoperative and the post-GBR, with a maximum deviation discrepancy of 3.4 mm (Li et al., 2021). Another study recorded an accuracy rate of 95.82% (88.53%–99.15%) with meshes bent on stereolithographic models (Pellegrino et al., 2021). This value resulted from comparing the digitally calculated volumes added to the model from preoperative and postoperative CT scans. Comparing the two studies, the

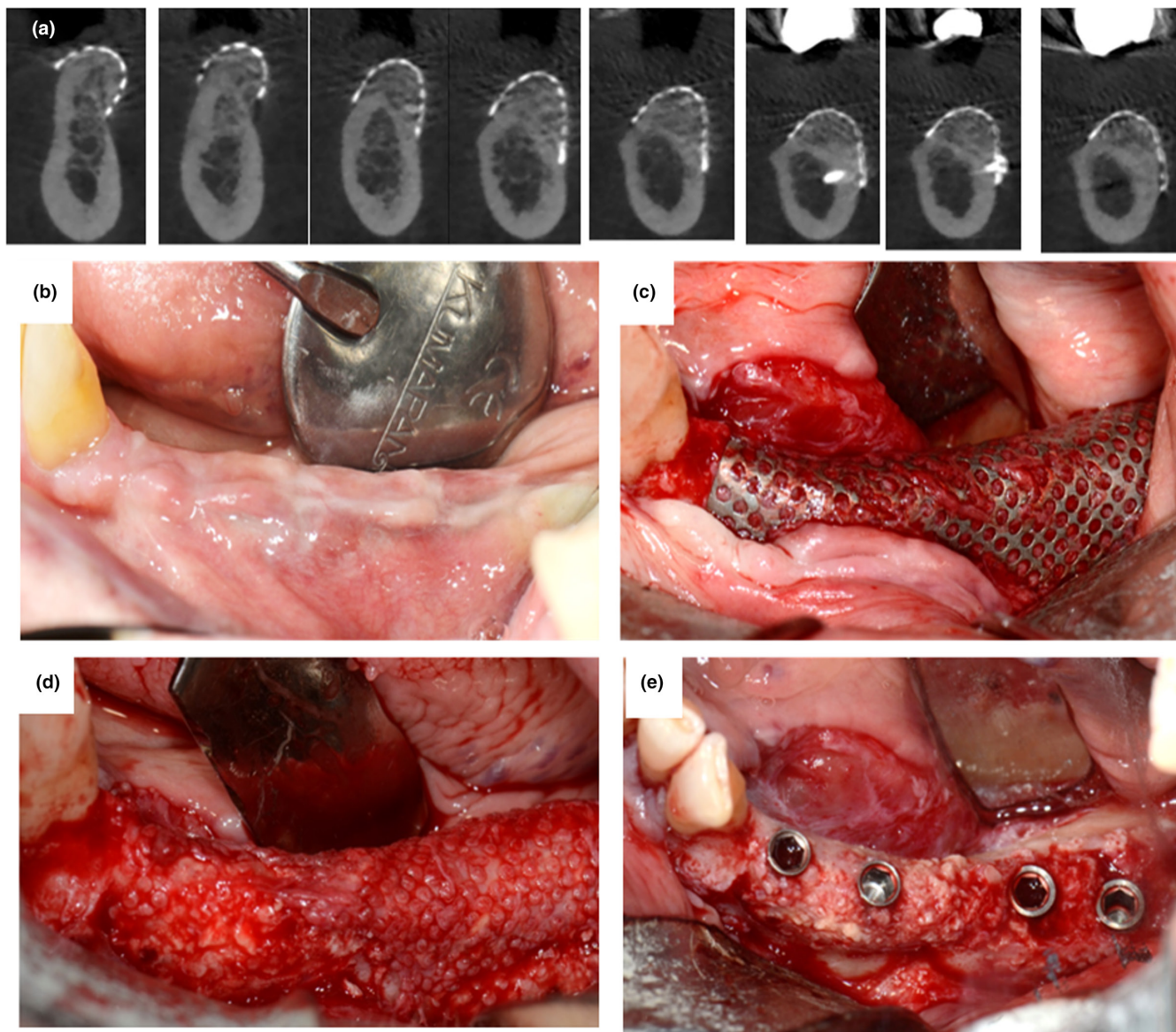


FIGURE 7 Postoperative cone-beam CT (a) and surgical re-entry with implant placement after mesh removal (b–e)

precision of a traditional mesh modeled on a virtually reconstructed defect is much greater than that of the printed one. The rest of the literature declared a perfect fitting of the meshes with no objective support or proof of this statement. Realistically, apart from the expertise of the operators, the quality of the fitting could depend significantly on the defect's characteristics. Since the postoperative data were obtained by a CBCT taken just before the implant placement, our study, as in Li et al. (Li et al., 2021), cannot be excluded the possibility of the mesh shifting during the healing period due to muscular activity, any complications that occurred, the wearing of a complete denture in case of total edentulism, or the loss of stabilization power of the fixation screws. Conversely, taking a CT scan just after the surgical intervention appears to be an ethical and scientifically valid evaluation method.

In terms of bone regeneration predictability, this study obtained an overall lower percentage of bone reconstruction (65%) than

the 69.8% of reconstructed bone volumes pretrimmed on stereolithographic model meshes by the same research team (Lizio et al., 2014). This reconstruction percentage rose to 88.2% excluding the failed cases, appearing close to 89% (892mm<sup>3</sup> of reconstructed bone out of 984mm<sup>3</sup> planned) of the Cucchi et al. study (Cucchi et al., 2020) and 91.9% (1.37 cc of 1.49 cc) of the Chiapasco et al. study (Chiapasco et al., 2021). The bone reconstruction percentage standard deviation of  $\pm 8.32$  (disregarding failure cases) was lower than the  $\pm 19.7$  reported by Lizio et al. (Lizio et al., 2014). It seems that when the exposure complication is manageable, appearing after about a month since the intervention and without signs of infection, the CAD/CAM GBR approach is reliable in fulfilling preoperatively plans, homogenizing the outcomes. As aforementioned, Li et al. reported a mean actual bone augmentation of 95.82% in virtual meshes compared with traditional meshes, including cases with implants located contextually to GBR (Pellegrino et al., 2021). [Correction added on

**FIGURE 8** Mesh fitting evaluation. A backward shift appears evident in the postoperative situation (b) regarding the virtual planning phase (a)

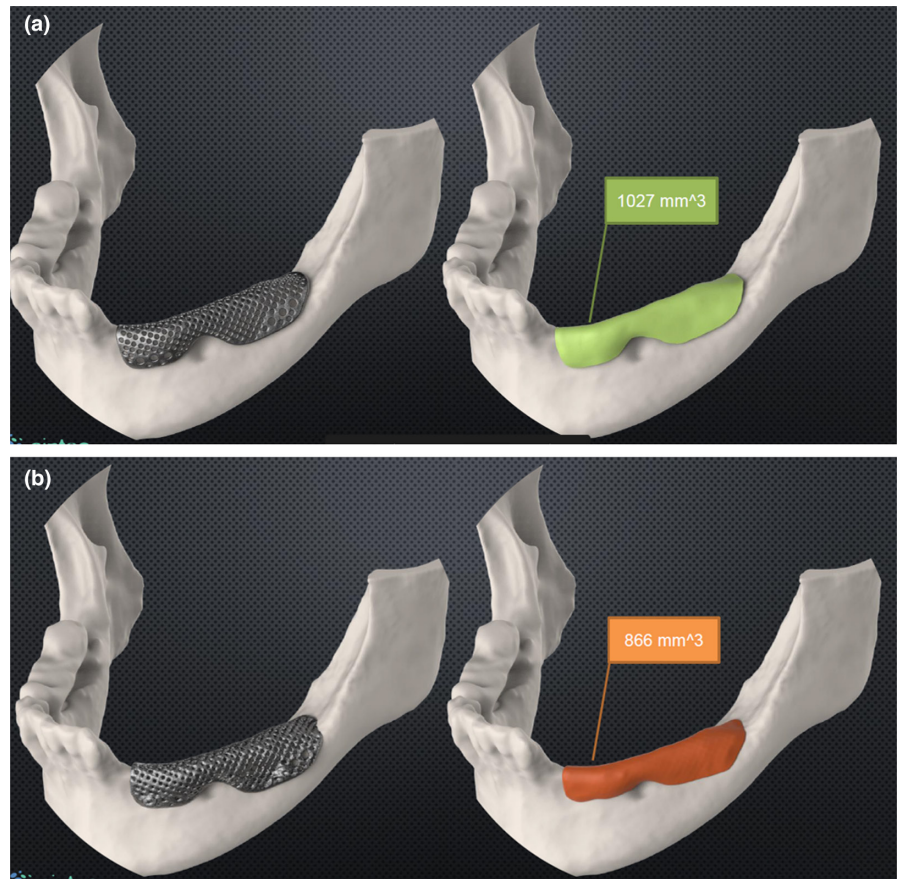


**TABLE 2** Patients' (Pts) data elaborated by comparison of postoperative cone-beam CT with preoperative one and virtual planning

Pts	Sites	Mesh fitting (%)	Planned bone volume (mm <sup>3</sup> )	Lacking bone volume (mm <sup>3</sup> )	Reconstructed bone Volume (mm <sup>3</sup> )	Reconstructed bone Volume (%)
1	1	83.61	823.4	65.34	758.11	92.07
2	2	83.83	1073.25	152.73	920.52	85.77
3	3					0
4	4	71.64	693.19	16.15	677.04	97.67
5	5					0
6	6	69.92	1864.52	30.72	1833.8	98.35
7	7	72.07	884.68	22.34	862.34	97.47
8	8	87.21	1642.47	498.88	1143.59	69.63
9	9	100	507.04	89.89	417.15	82.27
9	10					0
10	11	90.14	791.74	104.29	687.45	86.83
10	12					0
11	13		1012	160	852	84.19
12	14	84.32	1419	110	1309	92.25
13	15	99.74	1362	70	1292	94.86
14	16	88.15	718.07	63.02	655.05	91.22
15	17	53.33	2619.13	407	2012.13	76.82
16	18					0
17	19	83.08	735.01	100.3	634.71	86.35

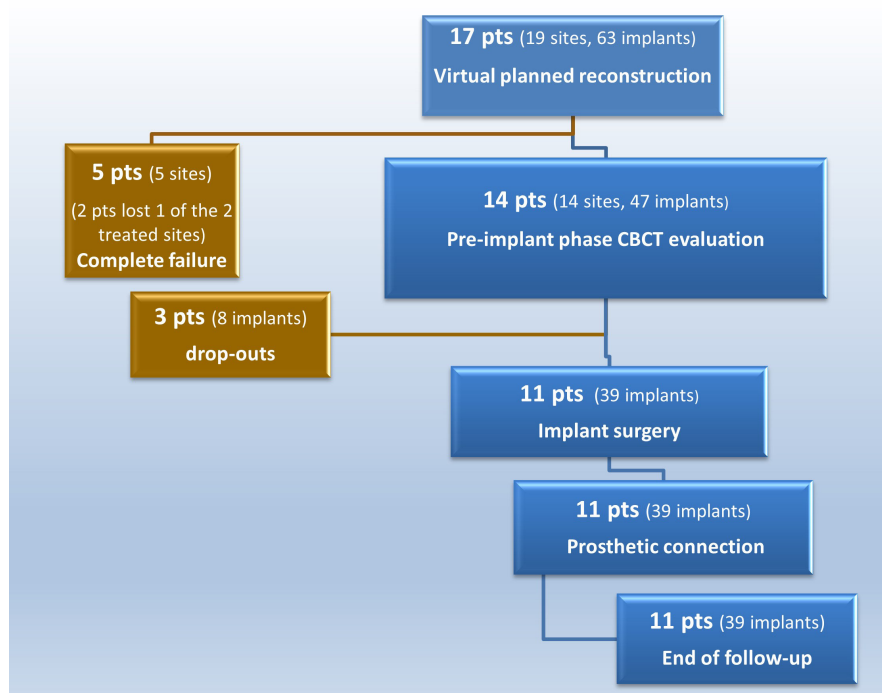
**TABLE 3** Mean values of the patients' data elaborated by comparison of postoperative cone-beam CT with preoperative one and virtual planning

Variable	Mean ± SD	Minimum	Maximum
Mesh fitting %	82 ± 13.4	53.3	100
Planned bone volume (mm <sup>3</sup> )	1153.25 ± 577.78	507.04	2619.13
Lacking bone volume (mm <sup>3</sup> )	149.33 ± 177.59	16.15	607
Reconstructed bone volume (mm <sup>3</sup> )	1003.92 ± 465.79	417.15	2012.13
Reconstructed bone volume %	65.04 ± 40.55 (including failures)	0	98.35
	88.2 ± 8.32 (excluding failures)	69.63	98.35

**TABLE 4** Multivariate regression model results with RBV (Reconstructed Bone Volume) as dependent variable

RBV	Coef.	Std. Err.	t	p >  t	[95% Conf.]	Interval
Lower jaw	-51.0599	38.29294	-1.33	.204	-133.1901	31.07029
Posterior	40.2526	36.8771	1.09	.293	-38.84091	119.3461
Absence of exposure	53.1282	19.45283	2.73	.016	11.40602	94.85038
Absence of infection	9.527285	24.558	0.39	.704	-43.14438	62.19895
Cons <sup>a</sup>	35.9895	22.81047	1.58	.137	-12.93408	84.91309

<sup>a</sup>Constant (Y intercept) values.



**GRAPH 1** Patients' treatment flowchart

29th April 2022 after first online publication: The sentence 'This reconstruction percentage rose to 88.2%, excluding the failed cases (892mm<sup>3</sup> of reconstructed bone out of 984mm<sup>3</sup> planned) of the Cucchi et al. study (Cucchi et al., 2020) and 91.9% (1.37 of 1.49 cc) of the Chiapasco et al. study (Chiapasco et al., 2021)'. has been corrected to 'This reconstruction percentage rose to 88.2% excluding the failed cases, appearing close to 89% (892mm<sup>3</sup> of reconstructed bone out of 984mm<sup>3</sup> planned) of the Cucchi et al. study (Cucchi et al., 2020) and 91.9% (1.37 cc of 1.49 cc) of the Chiapasco et al. study (Chiapasco et al., 2021)' in this current version.]

The present study adopted the volumetric measurement for two main reasons. First, the radiologists who circumscribed the CT slices were unaware of the implant position, working independently from different competencies in the digital designer group. Second, since an overall superimposition of 82% (53%–100%) was recorded between the virtual and the postoperative mesh positions and dimensions, a linear comparison between the virtual-planned and postoperative bone height and width in the same implant zone would not have been possible. This issue is particularly evident in the case of forward or backward shifting. Indeed, all of the linear

evaluations reported in the literature existing were not compared with the planned evaluations (Ciocca et al., 2018).

The present study included the segmentation of the entire bone under the mesh, including the residual bone, being easier to define according to the grayscale nuances perceptible to the naked eye. A more reliable evaluation could have considered a digital analysis of the pixel grayscale values. Still, the lack of correspondence between the pixel data and the grayscale Hounsfield data for cone-beam CT exam algorithms prevented an objective digital radiological evaluation.

The overall 52.3% of exposures reported in the present study is less than the 70 (Lizio et al., 2016) - 80% (Lizio et al., 2014) reported by Lizio et al., but greater than the mean value of 34.8% among studies on traditional titanium GBR meshes (Briguglio et al., 2019) and within the reported range (10%–66%) of the CAD/CAM technique (Chiapasco et al., 2021; Ciocca et al., 2018; Cucchi et al., 2020; Hartmann et al., 2019; Sagheb et al., 2017). Indeed, in the present trial, such a problem significantly compromised the procedure, with five complete failures. Two authors (Hartmann & Seiler, 2020) reported 25% of exposures: 16% minimal, 7% "like one tooth width," and 1.5% complete. It is interesting to note the heterogeneity of the treated defects in the same trial, ranging from monoedentulism with immediate implant placement to complete edentulism. Hartman et al. (Hartmann et al., 2019), on 70 heterogeneous treated sites, reported 37% of exposures. The starting bone defect extension and the soft tissue characteristics declared crucial in conditioning the GBR (Cucchi et al., 2019; Miyamoto et al., 2012; Urban et al., 2021) seemed irrelevant to CAD/CAM treatments in the current literature. Multiple complex defects requiring specialized technological support were selected in this prospective trial. The actual extension of the defects has been verified by this paper's mean virtual-planned bone volume (1153 mm<sup>3</sup>), and by the number of implants (63 at 19 sites). For example, Li et al. (Li et al., 2021), recording a statistically significant customized mesh misfitting, reported a mesh exposure of 25% with a mean planned volume of 636.20 ± 341.18, with 20 implants placed at 16 sites. No relevance of the site's location came out from the multivariate analysis, following the literature; anyway, it is worth underlining that the limited sample size conditioned the importance of this datum.

The lack of uniqueness of a single expert operator could explain the failure recorded in the present paper, particularly regarding the management of soft tissues associated with the complexity and extension of defects with different localizations and characteristics. The reduced sample size did not permit correlation of the outcomes with each single operator skill. However, the operators were part of the same surgical team and school, with more than 10 years of surgical practice. From this point of view, it would have been helpful to enroll cases treated by the same surgeon, maybe with a reduced experience, to better comprehend the relevance of the variable of the learning curve in conditioning the final result. On the other hand, by providing expert prosthodontists and medical device designers with a more advanced level of training in the process, the ability of a single operator may not be mandatory.

A vestibular approach was adopted in literature instead of the mid-crestal one to keep the suture away from the grafted ridge zone and the mesh. Even if this incision did not statistically influence the exposure rate (Hartmann et al., 2019; Hartmann & Seiler, 2020; Sagheb et al., 2017), it could have reduced, in expert operators' hands, the rate of exposures encountered in the present trial, limiting, in addition, the mobilization of the soft tissues.

No covering of the augmented sites with a collagen membrane or platelet-rich plasma (PRP) or platelet-rich-fibrin (PRF) was adopted in this trial since their usefulness was not demonstrated yet. (Cucchi et al., 2021; Torres et al., 2010). Two cases consisted of completely edentulous maxillary atrophies, with a period of 2 weeks of postoperative healing before wearing a relined denture for esthetic purposes only. The other three failed sites were all in the posterior mandible, considered a problematic region for releasing soft tissues and maintaining tight closure, particularly in intermediate edentulism (one case) for the closeness of the teeth and their periodontal sulcus (Cucchi et al., 2019). Using a manually preformed, 0.2 mm-thick mesh could enable the surgeon to modify the mesh's shape intraoperatively in case of discrepancy between the digitally printed and actual clinical models, such as in the case of an intra-operative accident. A customized mesh is impractically larger for use in the laser-sintering process and does not allow for extemporaneous modifications. As in all systems requiring precision, a minimal procedural error can result in high costs to resolve.

Two controlled trials compared CAD/CAM meshes with pre-shaped ones. Sumida et al. (Sumida et al., 2015) treated defects with contextual implant placement, demonstrating the reduced operative time and exposure in the CAD/CAM group. Mounir et al. (Mounir et al., 2019) compared a pre-shaped titanium mesh on a stereolithographic model with a polyether ether ketone (PEEK) device and found no significant difference. A recent systematic review reported a 31% exposure rate, compared to a 51% rate using customized and traditional meshes (Zhou et al., 2021).

The digitally projected and printed meshes present the practical advantages of shortening the operation time, reducing the fixation screws, and obtaining rounded, blunt edges to make contact with the bone profile with minor damage to the soft tissues (Xie et al., 2020). Regarding the shortcomings of this approach, the costs of the mesh, estimated to be about \$425 (USD) by Ciocca et al., and the training for the management software must be considered (Ciocca et al., 2018).

Criticisms of the present study may include the limited number of cases, lack of statistical evaluation of the assessor's reliability of the mesh fitting and bone volumes, lack of proper assessment of the soft tissue features and the heterogeneity of the site localization. In our experience, digital GBR should currently be limited to complex cases and not be combined with other grafting techniques such as residual bone quantity and quality analysis, vascularization, and soft tissue availability. Future studies using broader sample size and reliable evaluation methods can further increase knowledge of this topic.

## 5 | CONCLUSIONS

The use of virtually planned GBR for extended 3D defects with customized meshes improved the predictability of bone regeneration by up to 88% in about 74% of the cases. The complete failure of five sites out of 19 for early exposures and infection could support an investigation into the relevance of anatomical features, surgical management, and improvement of the planning workflow.

### ACKNOWLEDGEMENTS

The authors thank Dr Andrea Sandi (Sintac, Biomedical Engineering, Rovereto, Italy) for his valuable work in CAD and the rapid prototyping of the customized devices and mesh fitting evaluation in collaboration with Dr Fabio Michelon. Open Access funding provided by Università degli Studi di Bologna within the CRUI-CARE Agreement. [Correction added on 14 May 2022, after first online publication: CRUI-CARE funding statement has been added.]

### CONFLICT OF INTEREST

No conflict of interest and no financial support.

### AUTHOR CONTRIBUTIONS

Giuseppe Lizio contributed to conceptualization (lead); formal analysis (supporting); investigation (lead); methodology (equal); supervision (equal); writing—original draft (lead); writing—review and editing (lead). Gerardo Pellegrino contributed to investigation (equal); formal analysis (supporting); methodology (equal). Giuseppe Corinaldesi: investigation (equal); methodology (equal); supervision (equal). Agnese Ferri contributed to conceptualization (supporting); data curation (lead); methodology (equal). Claudio Marchetti contributed to investigation (equal); supervision (lead). Pietro Felice contributed to methodology (equal); supervision (lead).

### DATA AVAILABILITY STATEMENT

Data available on request due to privacy/ethical restrictions.

### ORCID

Giuseppe Lizio  <https://orcid.org/0000-0002-7552-7523>

### REFERENCES

- Bartnikowski, M., Vaquette, C., & Ivanovski, S. (2020). Workflow for highly porous resorbable custom 3D printed scaffolds using medical grade polymer for large volume alveolar bone regeneration. *Clinical Oral Implants Research*, 31(5), 431–441. <https://doi.org/10.1111/clr.13579>
- Briguglio, F., Falcomatà, D., Marconcini, S., Fiorillo, L., Briguglio, R., & Farronato, D. (2019). The use of titanium mesh in guided bone regeneration: A systematic review. *International Journal of Dentistry*, 2019, 9065423. <https://doi.org/10.1155/2019/9065423>
- Chiapasco, M., Casentini, P., Tommasato, G., Dellavia, C., & Del Fabbro, M. (2021). Customized CAD/CAM titanium meshes for the guided bone regeneration of severe alveolar ridge defects: Preliminary results of a retrospective clinical study in humans. *Clinical Oral Implants Research*, 32(4), 498–510. <https://doi.org/10.1111/clr.13720>
- Chiapasco, M., Casentini, P., & Zaniboni, M. (2009). Bone augmentation procedures in implant dentistry. *International Journal of Oral and Maxillofacial Implants*, 24(Suppl), 237–259.
- Ciocca, L., Lizio, G., Baldissara, P., Sambuco, A., Scotti, R., & Corinaldesi, G. (2018). Prosthetically CAD-CAM-guided bone augmentation of atrophic jaws using customized titanium mesh: Preliminary results of an open prospective study. *Journal of Oral Implantology*, 44(2), 131–137. <https://doi.org/10.1563/aaid-joi-D-17-00125>
- Ciocca, L., Ragazzini, S., Fantini, M., Corinaldesi, G., & Scotti, R. (2015). Work flow for the prosthetic rehabilitation of atrophic patients with a minimal-intervention CAD/CAM approach. *Journal of Prosthetic Dentistry*, 114(1), 22–26. <https://doi.org/10.1016/j.prosdent.2014.11.014>
- Cucchi, A., Bianchi, A., Calamai, P., Rinaldi, L., Mangano, F., Vignudelli, E., & Corinaldesi, G. (2020). Clinical and volumetric outcomes after vertical ridge augmentation using computer-aided-design/computer-aided manufacturing (CAD/CAM) customized titanium meshes: A pilot study. *BMC Oral Health*, 20(1), 219. <https://doi.org/10.1186/s12903-020-01205-4>
- Cucchi, A., Chierico, A., Fontana, F., Mazzocco, F., Cinquegrana, C., Belleggia, F., Rossetti, P., Soardi, C. M., Todisco, M., Luongo, R., Signorini, L., Ronda, M., & Pistilli, R. (2019). Statements and recommendations for guided bone regeneration: Consensus report of the guided bone regeneration symposium held in Bologna, October 15 to 16, 2016. *Implant Dentistry*, 28(4), 388–399. <https://doi.org/10.1097/id.0000000000000909>
- Cucchi, A., Vignudelli, E., Franceschi, D., Randellini, E., Lizio, G., Fiorino, A., & Corinaldesi, G. (2021). Vertical and horizontal ridge augmentation using customized CAD/CAM titanium mesh with versus without resorbable membranes. A randomized clinical trial. *Clinical Oral Implants Research*, 32(12), 1411–1424. <https://doi.org/10.1111/clr.13841>
- Hartmann, A., Hildebrandt, H., Schmohl, J. U., & Kämmerer, P. W. (2019). Evaluation of risk parameters in bone regeneration using a customized titanium mesh: Results of a clinical study. *Implant Dentistry*, 28(6), 543–550. <https://doi.org/10.1097/id.0000000000000933>
- Hartmann, A., & Seiler, M. (2020). Minimizing risk of customized titanium mesh exposures - a retrospective analysis. *BMC Oral Health*, 20(1), 36. <https://doi.org/10.1186/s12903-020-1023-y>
- Jacotti, M., Barausse, C., & Felice, P. (2014). Posterior atrophic mandible rehabilitation with onlay allograft created with CAD-CAM procedure: A case report. *Implant Dentistry*, 23(1), 22–28. <https://doi.org/10.1097/id.0000000000000023>
- Li, L., Wang, C., Li, X., Fu, G., Chen, D., & Huang, Y. (2021). Research on the dimensional accuracy of customized bone augmentation combined with 3D-printing individualized titanium mesh: A retrospective case series study. *Clinical Implant Dentistry and Related Research*, 23(1), 5–18. <https://doi.org/10.1111/cid.12966>
- Lizio, G., Corinaldesi, G., & Marchetti, C. (2014). Alveolar ridge reconstruction with titanium mesh: A three-dimensional evaluation of factors affecting bone augmentation. *International Journal of Oral and Maxillofacial Implants*, 29(6), 1354–1363. <https://doi.org/10.11607/jomi.3417>
- Lizio, G., Mazzone, N., Corinaldesi, G., & Marchetti, C. (2016). Reconstruction of extended and morphologically varied alveolar ridge defects with the titanium mesh technique: Clinical and dental implants outcomes. *The International Journal of Periodontics & Restorative Dentistry*, 36(5), 689–697. <https://doi.org/10.11607/prd.2447>
- Maiorana, C., Santoro, F., Rabagliati, M., & Salina, S. (2001). Evaluation of the use of iliac cancellous bone and anorganic bovine bone in the reconstruction of the atrophic maxilla with titanium mesh: A clinical and histologic investigation. *International Journal of Oral and Maxillofacial Implants*, 16(3), 427–432.

- Miyamoto, I., Funaki, K., Yamauchi, K., Kodama, T., & Takahashi, T. (2012). Alveolar ridge reconstruction with titanium mesh and autogenous particulate bone graft: Computed tomography-based evaluations of augmented bone quality and quantity. *Clinical Implant Dentistry and Related Research*, 14(2), 304–311. <https://doi.org/10.1111/j.1708-8208.2009.00257.x>
- Mounir, M., Shalash, M., Mounir, S., Nassar, Y., & El Khatib, O. (2019). Assessment of three dimensional bone augmentation of severely atrophied maxillary alveolar ridges using prebent titanium mesh vs customized poly-ether-ether-ketone (PEEK) mesh: A randomized clinical trial. *Clinical Implant Dentistry and Related Research*, 21(5), 960–967. <https://doi.org/10.1111/cid.12748>
- Pellegrino, G., Lizio, G., Ferri, A., & Marchetti, C. (2021). Flapless and bone-preserving extraction of partially impacted mandibular third molars with dynamic navigation technology. A report of three cases. *International Journal of Computerized Dentistry*, 24(3), 253–262.
- Pieri, F., Corinaldesi, G., Fini, M., Aldini, N. N., Giardino, R., & Marchetti, C. (2008). Alveolar ridge augmentation with titanium mesh and a combination of autogenous bone and anorganic bovine bone: A 2-year prospective study. *Journal of Periodontology*, 79(11), 2093–2103. <https://doi.org/10.1902/jop.2008.080061>
- Poomprakobsri, K., Kan, J. Y., Rungcharassaeng, K., & Lozada, J. (2021). Exposure of barriers used in GBR: Rate, timing, management, and its effect on grafted bone. A retrospective analysis. *Journal of Oral Implantology*. <https://doi.org/10.1563/aaid-joi-D-19-00252>. Online ahead of print.
- Sagheb, K., Schiegnitz, E., Moergel, M., Walter, C., Al-Nawas, B., & Wagner, W. (2017). Clinical outcome of alveolar ridge augmentation with individualized CAD-CAM-produced titanium mesh. *International Journal of Implant Dentistry*, 3(1), 36. <https://doi.org/10.1186/s40729-017-0097-z>
- Sanz, M., Dahlin, C., Apatzidou, D., Artzi, Z., Bozic, D., Calciolari, E., De Bruyn, H., Dommisch, H., Donos, N., Eickholz, P., Ellingsen, J. E., Haugen, H. J., Herrera, D., Lambert, F., Layrolle, P., Montero, E., Mustafa, K., Omar, O., & Schliephake, H. (2019). Biomaterials and regenerative technologies used in bone regeneration in the craniomaxillofacial region: Consensus report of group 2 of the 15th European workshop on periodontology on bone regeneration. *Journal of Clinical Periodontology*, 46(Suppl 21), 82–91. <https://doi.org/10.1111/jcpe.13123>
- Sumida, T., Otawa, N., Kamata, Y. U., Kamakura, S., Mtsushita, T., Kitagaki, H., Mori, S., Sasaki, K., Fujibayashi, S., Takemoto, M., Yamaguchi, A., Sohamura, T., Nakamura, T., & Mori, Y. (2015). Custom-made titanium devices as membranes for bone augmentation in implant treatment: Clinical application and the comparison with conventional titanium mesh. *Journal of Cranio-Maxillo-Facial Surgery*, 43(10), 2183–2188. <https://doi.org/10.1016/j.jcms.2015.10.020>
- Torres, J., Tamimi, F., Alkhraisat, M. H., Manchón, A., Linares, R., Prados-Frutos, J. C., Hernández, G., & López Cabarcos, E. (2010). Platelet-rich plasma may prevent titanium-mesh exposure in alveolar ridge augmentation with anorganic bovine bone. *Journal of Clinical Periodontology*, 37(10), 943–951. <https://doi.org/10.1111/j.1600-051X.2010.01615.x>
- Urban, I. A., Saleh, M. H. A., Ravidà, A., Forster, A., Wang, H. L., & Barath, Z. (2021). Vertical bone augmentation utilizing a titanium-reinforced PTFE mesh: A multi-variate analysis of influencing factors. *Clinical Oral Implants Research*, 32(7), 828–839. <https://doi.org/10.1111/clr.13755>
- Xie, Y., Li, S., Zhang, T., Wang, C., & Cai, X. (2020). Titanium mesh for bone augmentation in oral implantology: Current application and progress. *International Journal of Oral Science*, 12(1), 37. <https://doi.org/10.1038/s41368-020-00107-z>
- Zhou, L., Su, Y., Wang, J., Wang, J., Wang, X., & Liu, Q. (2021). Effect of exposure rates with customized versus conventional titanium mesh on guided bone regeneration: A systematic review and meta-analysis. *Journal of Oral Implantology*. <https://doi.org/10.1563/aaid-joi-D-20-00200>. Online ahead of print.

#### SUPPORTING INFORMATION

Additional supporting information may be found in the online version of the article at the publisher's website.

**How to cite this article:** Lizio, G., Pellegrino, G., Corinaldesi, G., Ferri, A., Marchetti, C., & Felice, P. (2022). Guided bone regeneration using titanium mesh to augment 3-dimensional alveolar defects prior to implant placement. A pilot study. *Clinical Oral Implants Research*, 33, 607–621. <https://doi.org/10.1111/clr.13922>